Ultrasonics Sonochemistry 73 (2021) 105502

Contents lists available at ScienceDirect

Ultrasonics Sonochemistry

journal homepage: www.elsevier.com/locate/ultson

# Ultrasonic-assisted catalytic transfer hydrogenation for upgrading pyrolysis-oil

Ethan Struhs [a], Samuel Hansen [a], Amin Mirkouei [a,*], Maria Magdalena Ramirez-Corredores [b], Kavita Sharma [c], Robert Spiers [c], John H. Kalivas [c]

[a] Department of Mechanical Engineering, University of Idaho, Idaho Falls, ID 83402, USA
[b] Energy and Environment S&T Division, Idaho National Laboratory, Idaho Falls, ID 83401, USA
[c] Department of Chemistry, Idaho State University, Pocatello, ID 83204, USA

ARTICLE INFO

*Keywords:*
Ultrasonic cavitation
Catalytic transfer hydrogenation
Upgrading
Pyrolysis oil
Sonotreatment

ABSTRACT

Recent interest in biomass-based fuel blendstocks and chemical compounds has stimulated research efforts on conversion and upgrading pathways, which are considered as critical commercialization drivers. Existing pre-/post-conversion pathways are energy intense (e.g., pyrolysis and hydrogenation) and economically unsustainable, thus, more efficient process solutions can result in supporting the renewable fuels and green chemicals industry. This study proposes a process, including biomass conversion and bio-oil upgrading, using mixed fast and slow pyrolysis conversion pathway, as well as sono-catalytic transfer hydrogenation (SCTH) treatment process. The proposed SCTH treatment employs ammonium formate as a hydrogen transfer additive and palladium supported on carbon as the catalyst. Utilizing SCTH, bio-oil molecular bonds were broken and restructured via the phenomena of cavitation, rarefaction, and hydrogenation, with the resulting product composition, investigated using ultimate analysis and spectroscopy. Additionally, an in-line characterization approach is proposed, using near-infrared spectroscopy, calibrated by multivariate analysis and modeling. The results indicate the potentiality of ultrasonic cavitation, catalytic transfer hydrogenation, and SCTH for incorporating hydrogen into the organic phase of bio-oil. It is concluded that the integration of pyrolysis with SCTH can improve bio-oil for enabling the production of fuel blendstocks and chemical compounds from lignocellulosic biomass.

## 1. Introduction

### 1.1. Challenges and motivation

Nowadays, renewable products (e.g., bioenergy) have been suggested as green and sustainable resources that have potentials to address major world challenges (e.g., fossil fuel reserve depletion and greenhouse gas emission). Currently, bioenergy production from various biomass feedstocks provides the largest portion (approximately 4.5% out of 10%) of renewable energy sources in the U.S. [1]. One of the most investigated pathways for producing fuel blendstocks and chemical compounds from biomass involves a thermochemical biomass conversion process, followed by upgrading steps that typically concern hydro-processing [2]. Bio-oil is an intermediate product from thermochemical conversion processes (e.g., pyrolysis or liquefaction) of biomass feedstocks [3,4]. Bio-oil in raw form can potentially be used as heating oil, however, bio-oil remains inequivalent to petroleum-based fuels due primarily to its lower heating value [5]. The lower heating value of bio-oil is associated with the high oxygen and water content, as well as the low hydrogen to carbon (H/C) ratio and high oxygen to carbon (O/C) ratio [6]. Some other bio-oil unwanted characteristics (e.g., viscosity, acidity, and thermal instability) preclude many potential applications [7]. Bio-blendstock production from bio-oil has been considered as a potential source of renewable products (bioproducts)

*Abbreviations:* ASTM, American Society for Testing and Materials; bpd, barrels per day; CS, corn stover; CTH, catalytic transfer hydrogenation; CV, cross-validation; H/C, hydrogen to carbon ratio; HDT, hydrotreatment; KF, Karl Fischer titration; LOOCV, leave-one-out cross-validation; LV, latent variables; NIR, near-infrared; NMR, nuclear magnetic resonance; O/C, oxygen to carbon ratio; Pd/C, palladium supported on carbon; PLS, partial least square; PW, pinewood; RMSEC, root-mean-square-error of calibration; RR, ridge regression; SCTH, sono-catalytic transfer hydrogenation; TH, transfer hydrogenation; UC, ultrasonic cavitation.

* Corresponding author at: University of Idaho, Tingey Administration Building, Suite 310, Idaho Falls 83402, USA.
*E-mail address:* amirkouei@uidaho.edu (A. Mirkouei).

https://doi.org/10.1016/j.ultsonch.2021.105502
Received 18 June 2020; Received in revised form 15 January 2021; Accepted 18 February 2021
Available online 23 February 2021

[8], however, the unwanted characteristics prevent long-term storage necessary for distribution at the commercial level [9,10]. Therefore, upgrading treatments (before storage and distribution) attempt to address bio-oil quality issues and improve usability and applicability.

### 1.2. Background

Thermochemical technologies (e.g., pyrolysis) can be designed to be feedstock flexible, while economic assessment demonstrated advantages for distributed processing (e.g., portable refineries) [11]. Depending on the operating conditions, pyrolysis can be categorized into two categories, namely slow and fast pyrolysis. In slow pyrolysis, biomass is heated up to a temperature of approximately 300–400 °C with a heating rate around 0.1–1 °C/s and residence time around 10–100 min. During the slow pyrolysis process, the vapors prolonged reaction leads to increased formation of solid char. Fast pyrolysis is operated at temperatures of 500–650 °C, heating rates of around 10–200 °C/s, and a residence time of below 2–10 s. Fast pyrolysis reactor technologies are varied in development (e.g., fluidized bed, auger type, and free-fall), each with unique advantages and disadvantages [12]. This study focuses on a free-fall reactor configuration, and the rationale behind free-fall pyrolysis reactor lies on the simple, robust design and control, high process yield, and minimal use of sweep gas, as well as being able to conveniently control and examine the kinetic parameters, mass balance, and residence time [13–15]. Fast pyrolysis processes produce 30–70 wt % of liquid product (bio-oil), 15–25 wt% of solid product (biochar), and 10–20 wt% of non-condensable gases, depending on various parameters, such as feedstock type and particle size, as well as whether or not a catalyst is used [16]. The main product of fast pyrolysis process is bio-oil, which is a precursor to bioproducts, using various upgrading processes [17]. Bio-oil upgrading can involve: (a) separating light, bio-distillate, and heavy fractions of bio-oil, (b) upgrading and stabilizing into oxygenated blendstocks, and (c) producing alternative renewable products [18,19]. The massive presence of oxygenated compounds has made hydrotreatment (HDT) an effective processing option for pursuing deoxygenation [20]. However, the required process severity (e.g., pressure, temperatures, and heat) of existing HDT technologies makes these processes cost intense and limits the application for using thermally unstable bio-oil [2]. Various physicochemical approaches are under development for bio-oil upgrading, e.g., electrochemical hydrogenation, electrocatalytic hydrogenation, catalytic transfer hydrogenation, and ultrasonic cavitation [2,21]. Table 1 compares the similarities and differences between prior published studies and this study based on the following applied physicochemical treatment approaches:

- Ultrasonic Cavitation (UC). Earlier studies focused on UC treatments (sono-treatment) and sonochemistry to treat petroleum-based oil and its fractions for mitigating some of oil issues, e.g., high viscosity, instability, and heteroatom removal [24]. Bio-oil properties (e.g., H/C and O/C ratios) have also been improved by UC treatments [31]. Vibration induced waves cause cavitation, which is the violent rise and collapse of air cavities within a fluid. These cavity implosions cause phenomena, such as sonoluminescence, thermal scission, rarefaction, radical formation, and bond cleavage, resulting internal temperatures of cavitation bubbles in water can reach up to 10,000 °C and pressures up to 2000 atmospheres. These conditions can be attained using commercially available ultrasonic processors. The induced extreme temperatures are capable of breaking heavy molecule bonds [24] and improving the reaction rate on a micro-scale [32]. Further details about sono-treatment for upgrading bio-oil or heavy oil are provided in earlier studies [22,23,25].
- Catalytic Transfer Hydrogenation (CTH). Bio-oil upgrading mainly involves its dewatering and deoxygenation. Deoxygenation is carried out by hydrogenation and hydrogenolysis, also known as hydrodeoxygenation [26]. Hydrogenation and hydrogenolysis reactions are the preferred approaches for correcting the inherent hydrogen deficiency of lignocellulosic-derived oil, removing heteroatomic moieties, and increasing their energy value. Transfer hydrogenation reactions are environmentally friendly, and function via transferring hydrogen from a hydrogen-donor compound (H-donor) to hydrogen-deficient compounds, using a low-temperature chemical reaction. Earlier studies reported that catalysts could enhance reactivity, and several catalysts have been used for bio-oil upgrading via CTH, such as ruthenium, palladium, and nickel [27,33]. Recent studies investigated the application of CTH for hydrogenation of vegetable oils (soybean oil) and model compounds present in bio-oil, which showed a promising pathway for upgrading [28,34]. The catalysts are selected to allow for a favorable interaction among the active site, the H-donor and the reacting H-deficient compounds. Expensive metallic catalysts could be cost-effective only if high activity and selectivity are accompanied by longevity and regenerability. The high activity of palladium and palladium supported on carbon (Pd/C) make them as the preferred catalysts that have been extensively used in hydrogenation reactions where recycling after a long run cycle is feasible [28,29].) Also, ammonium formate ($NH_4HCO_2$) is a commonly known H-donor that has been used for CTH treatment [22].
- Sono-Transfer Hydrogenation (STH) and Sono-Catalytic Transfer Hydrogenation (SCTH). Integrating CTH and UC with pyrolysis could lead to an intensified process of increased efficiency. Earlier studies explored the application of STH and SCTH in the selection of proper catalysts (e.g., titanium, palladium, and Ni-Mo-B amorphous) and H-donors, which were used on deoxygenation, hydrogenation, and hydrodeoxygenation, as well as the performance of these various catalysts and solvents [28,30]. The complex composition of bio-oil leads to a diverse range of reactivity that generates various issues on thermal stability, corrosivity, formation deposits, miscibility, or compatibility. The barriers in effectively upgrading bio-oil to bio-

**Table 1**
Prior upgrading studies, focusing on ultrasonic-assisted catalytic transfer hydrogenation.

| References | Pyrolysis | Treatment | | | Ultrasonic Cavitation | Sources | Catalyst | Hydrogen Donor |
|---|---|---|---|---|---|---|---|---|
| | | CTH | STH | SCTH | | | | |
| [22] | × | ✓ | × | × | × | Dry ice/solvent | Pd/C | Ammonium formate |
| [23] | × | × | × | × | ✓ | Microalgae | – | – |
| [24] | × | × | × | × | ✓ | Heavy gas oil | Metal sulfide | – |
| [25] | ✓ | × | × | × | ✓ | Pine Nut Shell | – | – |
| [26] | ✓ | ✓ | × | × | × | Microalgae | Zeolite | 2-propanol |
| [27] | × | ✓ | × | × | × | Furfural | Ru/C | 2-propanol |
| [28] | × | ✓ | × | × | ✓ | Soybean oil | Pd/C | Ammonium/potassium/sodium formats & formic acid |
| [29] | × | ✓ | × | × | × | Anthracene | Pd/C | Hydrogen gas |
| [30] | × | ✓ | ✓ | ✓ | ✓ | Diphenylacetylene | Pd/boehmite, Pd/$CeO_2$ | Hydrogen gas |
| This study | ✓ | ✓ | ✓ | ✓ | ✓ | Pinewood & corn stover | Pd/C | Ammonium formate |

blendstocks represent an urgent need that is not being resolved due to existing conversion intricacies and characterization limitations in today's experimental practices.

- In-line Characterization. Bio-oil characterization is challenging due to the complexity of its composition that includes compounds with a wide distribution of boiling points and molecular weight, and with different physicochemical characteristics, such as polarity, solubility, stability, and reactivity. Moreover, many of the bio-oil compounds are present at low concentrations. Therefore, detailed analysis requires a combination of several analytical methods. In-line characterization of untreated and treated bio-oil samples can provide insights for controlling the basic parameters H/C and O/C ratios associated with hydrogen donation in the proposed SCTH reactor. The constraints can be overcome through in-line bio-oil measurements, using analytical devices, as well as calibration and predicting modeling approaches [35–37].

### 1.3. Objective and scope

A review of literature shows that there are few published studies, using ultrasonic-assisted catalytic transfer hydrogenation treatments for upgrading bio-oil or heavy oil, using different catalysts and hydrogen donors. Therefore, this study proposed a pathway, including a mixed pyrolysis conversion process with UC, CTH, STH, and SCTH treatments, as well as an in-line characterization to better understand and predict the effects of reaction parameters (e.g., temperature, pressure, and catalysts). The primary objective of this study is to explore and empirically verify the effectiveness of the proposed approaches by characterizing samples of untreated and treated bio-oil, using various analytical methods, as detailed in the next section.

## 2. Experimental methods

The procedure in this study encompasses three main steps: (a) biomass pretreatment and pyrolysis conversion process, (b) UC, CTH, STH, and SCTH upgrading processes, and (c) bio-oil characterization and properties assessment (Fig. 1). The experimental details for biomass pretreatment processes (e.g., dewatering and size reduction) are included for completion purposes, but are not subject to the present work. We received various pretreated (dried and ground) biomass samples from Idaho National Lab, Bioenergy Feedstock Library, including detailed information about the biomass properties and components.

### 2.1. Conversion process

Samples of lignocellulosic biomass, i.e., pinewood (PW) and corn stover (CS), were converted by pyrolysis technology, employing a free-fall fast pyrolysis reactor that was specially designed for producing bio-oil, including multi-zone heating units with high adaptability. The conversion process operates at 400–600 °C temperatures, 10-15psi pressure, and residence time below two seconds (Table 2). Particularly, the customized pyrolysis setup includes an auto-feed system, free fall (5 feet) fast pyrolysis, and fixed-bed slow pyrolysis reactors, cyclones/separators, and condensers, as well as several controllers and solenoid valves (Fig. 2). Compressed nitrogen gas has been used to purge and maintain biomass flow, as well as control residence time during the conversion process. A cartridge heater pre-heats the feed flow and an external tape heater controls the conversion temperature of the reactor. Additionally, a solid copper coil is used internally in the reactor, for increasing biomass contact with heated elements via direct conduction, and to induce turbulence that extends the residence time (around 2 s). The results indicate that the copper coil primarily acts as a heat transfer element.

The instances of difficulties encountered during setting up and the general findings are in good agreement and confirm what have been reported by other researchers [38]. Bio-oil yield has been estimated from the weight of produced oil and the total amount of biomass fed to the reactor. The estimated average yield is based on the average yield after 3–5 experiments, each experiment includes five minutes of fast pyrolysis runs and 30 min of the slow pyrolysis process. The process yield range is 43-55 wt% bio-oil, 25-35 wt% biochar, and 10-20 wt% pyrolysis gas. The pyrolysis unit is a small-scale system with bio-oil losses throughout the operation process, which explains the observed lower yield, in comparison with typical pyrolysis yields reported by others (50–75%) [3].

### 2.2. Upgrading process

The studied SCTH treatment integrates ultrasonic processing with CTH approach, enabling operation under mild conditions and facilitating the upgrading of existing bio-oil characteristics (Fig. 3).

This study systematically investigates the impact of individual and combined UC, CTH, STH, and SCTH treatments. Bio-oil, catalyst, and ammonium formate were pre-weighed and added to the treatment vessel. Ultrasonic treatment was applied to the reacting mixture at 20 kHz and 50% amplitude. The sono-treatment was performed from 2.5 to 10 min of total time, using pulsed ultrasound. The pulse duration was

**Table 2**
Pyrolysis process parameters.

| Process Control | Set point | Average Value |
|---|---|---|
| Pre-heater (°C) | 200 | – |
| Core heater (°C) | 500–550 | – |
| Tape heater (°C) | 500–550 | – |
| Thermo-well probe (°C) | N/A | 500 |
| Gas flow rate (LPM) | 15–23 | 20 |
| Pressure (psi) | 10–15 | 12.5 |
| Condenser (°C) | 5 | 5 |
| Biomass particle size (mm) | 2 | ~2 |
| Copper coil (ft) | 10 | N/A |
| Residence time (sec) | 1–2 | 1.5 |

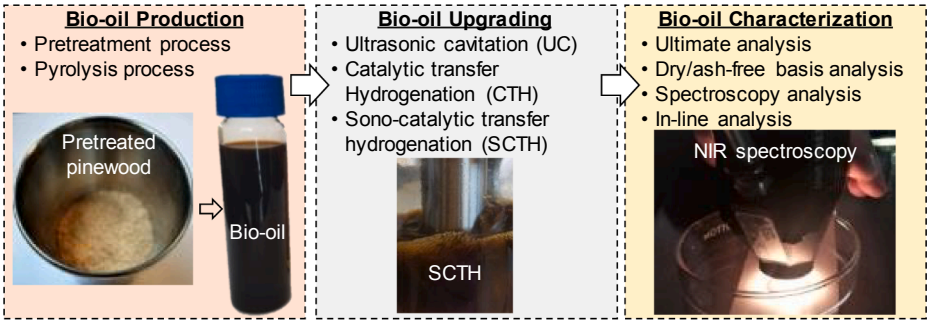


**Fig. 1.** Project procedure for bio-oil production, treatment, and assessment.

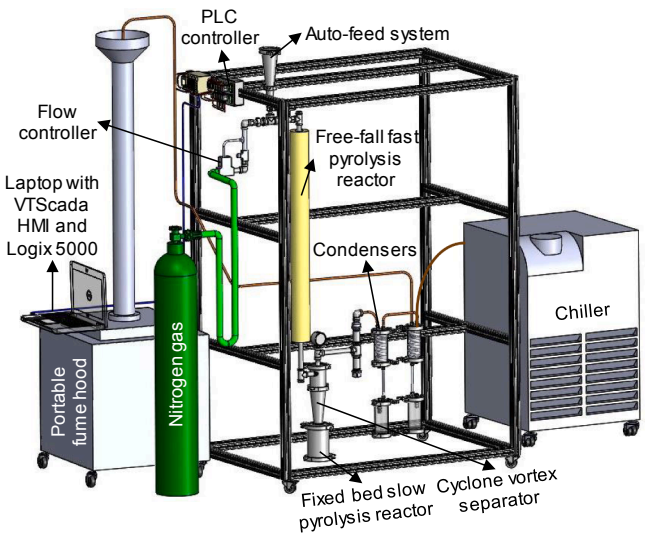


**Fig. 2.** A schematic of the custom-built fast and slow pyrolysis process for bio-oil production.

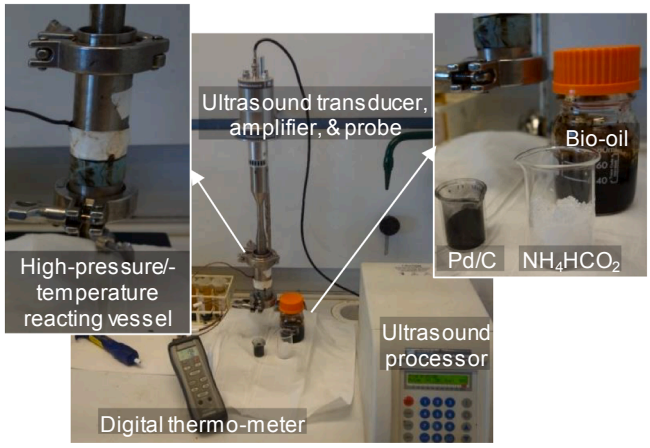


**Fig. 3.** Sono-catalytic transfer hydrogenation (SCTH) setup.

20sec and switching off the ultrasound for 59sec. Pulse mode operation is used to allow for intermittent and sufficiently cooling the ultrasonic vessel, and also preventing pressure build-up within the sealed vessel and reducing possible safety hazards, such as explosion.

Pd/C catalyst was used for promoting hydrogenation reactions, and the decomposition of H-donor ($NH_4HCO_2$). Pd/C catalyst has a nominal Pd content of about 1 wt% and was loaded to the reactor in an amount of 0.5 g. The effect of H-donor concentration was studied by varying its loading in the range from 2.5% to 15%. The sample nomenclature includes the duration of sono-treatment after "S" initial (sono-treatment) and the amount of H-donor after "TH" (transfer hydrogenation), notice also the presence of "C" for samples that have been treated under the combined SCTH treatment. For instance, PW-BO is an untreated PW bio-oil and PW-S10TH1.4 is the product of treating PW bio-oil with a sono-transfer-hydrogenation treatment under sonication for 10 min, 1.4 g of H-donor, and in the absence of catalyst. This study also investigated the effect of second-pass treatment (2S) for treated products of PW-S2.5CTH1.4, PW-S2.5CTH4.1, and PW-S2.5CTH6.9 by sampling 8–10 g for characterization purposes, and adding 8–10 g of raw bio-oil and additional 1.4 g $NH_4HCO_2$. An additional UC treatment was then applied for 2.5 more minutes. For 2S experiments, no make-up catalyst was added since most of Pd/C catalyst from the primary treatment remained in the treated product. Blank experimental runs were carried out to decouple sono-treatment from the effect of H-donation. Table 3 summarizes the testing conditions of each experiment.

### 2.3. Bio-oil characterization

Ultimate analysis of untreated and treated bio-oil samples, along with proton nuclear magnetic resonance (1H NMR) and near-infrared (NIR) spectra recording, were carried out on all samples. Total acid number, viscosity, flash point, oxidative stability, density, specific gravity, and relative acidity were evaluated, using the American Society for Testing and Materials (ASTM) standard methods on raw bio-oil, as presented in Table S1 of Supplementary Information. Preliminary results indicate that the flash point of our produced bio-oil is approximately 114 °C, and the viscosity is about 32 cSt. A comparison of some of these properties with that exhibited by a typical fossil diesel and fuel oil, some of which are part of the diesel or fuel oil specifications ASTM D975 and ASTM D396, respectively, clearly indicates the enormous needs for quality upgrading. For instance, ASTM D975 requires a flash point for the U.S. diesel (No. 2) of 52 °C or for fuel oil (No. 2) of 38 °C, which are lower than the tested bio-oil in this study. Meanwhile, the viscosity has to be reduced from 32 to 4.1 cSt.

1H NMR spectra of bio-oil samples were collected, using a JEOL JNM-ECX 300A FT NMR 300-MHz spectrometer at a frequency of 300 MHz. Corresponding spectral specimens are prepared by dissolving 200 mg of each bio-oil sample in 0.6 mL of deuterated DMSO. 1H spectra were acquired with a 90-degree pulse angle, a pulse delay of 5sec, spinner frequency of 20 Hz, and sweep width of 8,000 Hz across 32 transients. 100 scans were collected for each sample with 30 min acquisition times. The residual solvent signal of DMSO (2.5 ppm) was used as the internal reference. Quantification of different types of protons has been done based on percentage area of the peaks found for different regions corresponding to different types of compounds, e.g., alkanes, aliphatic α to heteroatom/unsaturation, ether or methoxyl, alkene, and alcohol. 1H NMR spectral integrations are divided into the following ranges: 0.8–1.2 ppm, 1.5–2 ppm, 3.1 ppm, 3.4–3.8 ppm, 4.2

**Table 3**
Primary and secondary treatment runs and experimental conditions.

| Sample ID | Bio-oil (g) | Sono-treatment Time (min)* | $NH_4HCO_2$ (g) | Pd/C (g) |
|---|---|---|---|---|
| **Primary SCTH experiments** | | | | |
| PW-BO | 55 | 0 | 0 | 0 |
| PW-S2.5 | 55 | 2.5 | 0 | 0 |
| PW-S2.5TH1.4 | 55 | 2.5 | 1.4 | 0 |
| PW-S2.5TH8.2 | 55 | 2.5 | 8.2 | 0 |
| PW-S10TH1.4 | 55 | 10 | 1.4 | 0 |
| PW-S2.5CTH1.4 | 55 | 2.5 | 1.4 | 0.5 |
| PW-S2.5CTH4.1 | 55 | 2.5 | 4.1 | 0.5 |
| PW-S2.5CTH6.9 | 55 | 2.5 | 6.9 | 0.5 |
| CS-BO | 55 | 0 | 0 | 0 |
| CS-S10C | 55 | 10 | 0 | 0.5 |
| CS-S10CTH1.4** | 55 | 10 | 1.4 | 0.5 |
| CS-S10TH1.4 | 55 | 10 | 1.4 | 0 |
| **Secondary SCTH experiments** | | | | |
| PW-2S5TH2.7 | 56.9 | (2.5) + 2.5 | (1.4) + 1.4 | 0 |
| PW-2S5TH5.5 | 59.6 | (2.5) + 2.5 | (4.1) + 1.4 | 0 |
| PW-2S5TH8.2 | 62.4 | (2.5) + 2.5 | (6.9) + 1.4 | 0 |

BO: raw (untreated) bio-oil; PW: pinewood; CS: corn stover; S#: sono-treatment; 2S#: second-pass sono-treatment during #min; TH#: transfer hydrogenation using #g of H-Donor; C: catalytic.

* The sono-treatment was performed from 2.5 to 10 min of total time, using pulsed ultrasound.

** Cryo test used an ice bath to prevent temperature and pressure increase inside the ultrasound vessel that acts to ensure the measured changes are not due to temperature and heat, and are from actual chemical reactions.

ppm, 5 ppm, and 8.2 ppm.

NIR spectra were recorded, using ASD portable spectroradiometer probe, and analyzed through multivariate calibration, e.g., partial least squares (PLS) and ridge regression (RR), and predicting modeling, e.g., leave-one-out cross-validation (LOOCV) with the objective of developing an in-line characterization approach to monitor bio-oil quality (e.g., H/C and O/C ratios) during the conversion and upgrading processes. For NIR spectra recording, bio-oil samples were poured into a plastic petri dish and placed on top of black background in a dark room. The probe was pointed down at the sample, interacted with materials, and returned to the detector. After contacting the bio-oil sample, only that radiation (which is transmitted through the sample) will be available to interact with the plastic petri dish. This also means that only the radiation that is transmitted through both the sample and plastic petri dish will be able to interact with the black background. If the wavelengths that reach the black background are reflected, the back up through the plastic petri dish and sample will only be those wavelengths that have not been absorbed by any of three materials or previously reflected by first two materials.

## 3. Results and discussion

### 3.1. Ultimate analysis

The results of blank experiments that carried out in the absence of H-donor and catalyst show almost no change in water content when untreated PW bio-oil is subjected only to sono-treatment. However, the water content increased when the sono-treatment was combined with the addition of H-donor. The increase was insignificant with a small addition (1.4 g) of H-donor, but it was much higher either with an extended application of sono-treatment from 2.5 to 10 min or with a more considerable addition of H-donor from 1.4 to 8.2 g. Meanwhile, the treated CS oil showed a slight increase in water content, concomitant with the lowest concentration of H-donor, constantly employed throughout all the testing runs (1.4 g). The increase in water content was the same regardless of whether bio-oil was subjected to SCTH or STH treatments. Table 4 presents the ultimate analysis results of raw and treated bio-oil samples.

The increase in water content of treated bio-oil samples determined by Karl Fischer titration (KF) analysis (Fig. 4a), using H-donor cannot be taken as conclusive for hydrogenation because its decomposition produces water and formamide, which may be contributing to water content values (R1). Similarly, the increase in hydrogen content with the changes determined by ultimate analysis (Fig. 4b), assuming that each mole of H-donor contributes with five H-atoms. The difference between the determined and the estimated content values would indicate whether or not the H-donor decomposition might be responsible for the changes observed. Additionally, the thermal decomposition of formamide into carbon monoxide and ammonia is also possible (R2), as well as the decomposition of ammonium formate into ammonia and formic acid (R3). Under UC conditions, it is unlikely that any formed CO would remain in the liquid phase (R2). Conversely, bio-oil acidity and high water content might facilitate ammonia dissolution (R3). In the case that formamide would not decompose under the treatment conditions, formate decomposition will lead to increases in N, H, O, and C contents, while sonication will lead to increase N, H, and O, but the decrease in C contents. In terms of formamide decomposition, the effects of H-donor addition on composition are similar to those caused by sonication, since in this case, CO formed from H-donor is stripped from the liquid phase by sonication.

$$NH_4HCO_2 \rightarrow NH_2HCO + H_2O \quad \text{(R1)}$$

$$NH_2HCO \rightarrow CO + NH_3 \quad \text{(R2)}$$

$$NH_4HCO_2 \rightarrow NH_3 + H_2CO_2 \quad \text{(R3)}$$

The water content of treated samples is always higher than the estimated to be caused by the formate decomposition, except for PW-S2.5CTH1.4 that involved the smallest amount of H-donor. The large water formation cannot be due exclusively to hydrogenation reactions, and most likely, a substantial contribution of carbon rejection (C-rejection) mechanism might be the case. The C-rejection mechanism is the selective removal of C-atoms (or C-enriched moieties) from hydrocarbonaceous macromolecules as those present in heavy oils and bitumen (e.g., asphaltenes) and occurring during thermolytic conversion. The C-rejection mechanism could be facilitated by simultaneous dehydroxylation reactions, responsible for water formation. However, C-rejection is responsible for char or coke formation instead of water formation. Additionally, dehydroxylation with dehydration is also responsible for water formation, occurring on thermochemical processes. The most abundant O-functional group in biomass is the hydroxo (–OH) group, upon which removal water is formed. With regards to the changes in hydrogen content (Fig. 4b), different values between the determined and estimated content cannot be associated with H-donor decomposition, mainly because ammonium formate contributes with five H-atoms per mole and should lead to increases in H-content while in some instances a decrease has been observed. Whichever decomposition reaction takes place (R1-3), most of the hydrogen will be retained by a basic species, either formamide or ammonia. Given the acid nature of bio-oil, there would be an acid-base interaction or reaction that leads to hydrogen retention in the liquid phase. Hence, there are no reasons to expect an H-content decrease.

### 3.2. Dry and ash-free basis analysis

The organic oil phase assessments indicate that the increase in water

**Table 4**
Ultimate analysis results.

| Sample ID | KF (%w/w) | Carbon (%w/w) | Hydrogen (%w/w) | Nitrogen (%w/w) | Oxygen (diff.) (%w/w) | Sulfur (%w/w) | Ash (%w/w) |
|---|---|---|---|---|---|---|---|
| PW-BO | 41.1 | 34.11 | 8.50 | 0.19 | 56.99 | 0.01 | 0.21 |
| PW-S2.5 | 41.2 | 46.15 | 7.70 | 0.18 | 45.44 | 0.01 | 0.53 |
| PW-S2.5TH1.4 | 41.9 | 31.30 | 8.73 | 0.67 | 59.24 | 0.01 | 0.06 |
| PW-S10TH1.4 | 48.1 | 25.10 | 9.11 | 1.95 | 63.74 | 0 | 0.10 |
| PW-S2.5TH8.2 | 46.3 | 25.18 | 8.93 | 2.99 | 62.89 | 0.01 | 0.05 |
| PW-S2.5CTH1.4 | 41.1 | 33.26 | 8.45 | 0.67 | 57.46 | 0.01 | 0.14 |
| PW-S2.5CTH4.1 | 47.3 | 25.55 | 9.03 | 1.43 | 63.88 | 0 | 0.10 |
| PW-S2.5CTH6.9 | 48.0 | 24.34 | 9.05 | 2.46 | 64.07 | 0 | 0.07 |
| PW-2S5CTH2.7 | 47.2 | 27.17 | 8.88 | 1.09 | 62.64 | 0.01 | 0.20 |
| PW-2S5CTH5.5 | 50.5 | 23.31 | 9.12 | 1.84 | 64.96 | 0.01 | 0.75 |
| PW-2S5CTH8.2 | 48.8 | 23.32 | 9.09 | 2.94 | 64.60 | 0 | 0.05 |
| CS-BO | 62.1 | 19.68 | 9.76 | 0.33 | 70.18 | 0.02 | 0 |
| CS-S10C | 63.0 | 19.71 | 9.49 | 0.35 | 70.39 | 0.02 | 0 |
| CS-S10CTH1.4 | 62.9 | 19.36 | 9.80 | 0.81 | 69.99 | 0.02 | 0 |
| CS-S10TH1.4 | 63.1 | 18.87 | 9.82 | 0.80 | 70.46 | 0.02 | 0 |

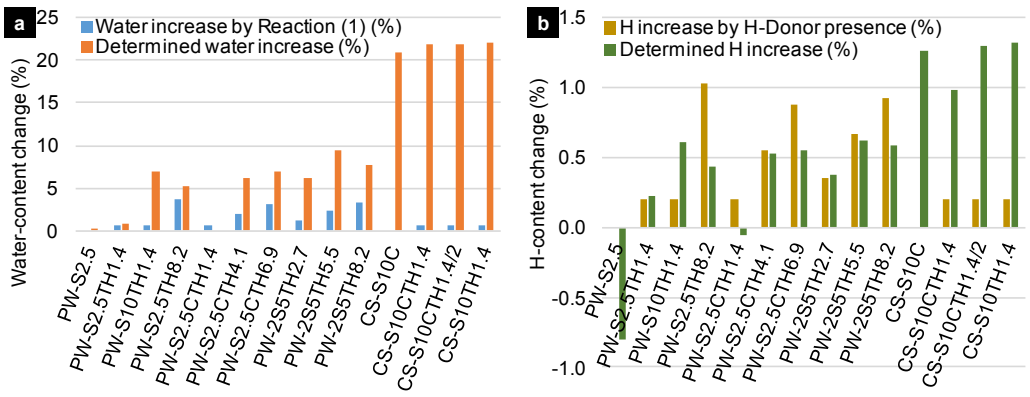


**Fig. 4.** Effects of H-donor addition and comparison of estimated and determined changes: (a) water content change and (b) H-content change.

content is accompanied by increases in N and O, decreases in C, and random changes in H. Thus, the changes in C and H on the elemental composition normalized to dry and ash-free bases in the organic phase (Table 5).

The dry/ash-free basis data is used to calculate and assess H/C and O/C ratios as the key upgrading factors and function of H-donor concentration in the reacting medium for different treatment conditions. Fig. 5 represents a graphical comparison of H/C ratio gains among different treatments and conditions, seeking pieces of evidence that could show any potential synergies among sono-treatments with hydrogen transfer reactions (e.g., STH). At first glance, it is evident that the effect of an exclusive sono-treatment is to downgrade the oil with a drastic decrease of H/C ratio (the comparison of PW-BO and PW-S2.5 samples). The decrease of O/C ratio may indicate an apparent upgrade and the deoxygenated oil can be considered as upgraded, while it is still exhibiting an increased hydrogen deficiency.

Under STH and SCTH, H/C ratio is upgraded while O/C ratio is downgraded, which is consistent with the C-rejection mechanism, as observed in heavy oil sono-treatments [39]. STH results showed a similar level of upgrading with PW-S10TH1.4, i.e., low H-donor content (1.4 g)/long sonication time (10 min) and with high H-donor content (8.2 g)/low sonication time (2.5 min). Comparatively (samples PW-S10TH1.4, PW-2S2.5CTH5.1, and PW-S2.5CTH1.4), STH was tested at the longest time (10 min of UC pulses), particularly twice as long as 2SCTH (5 min of UC pulses) and four times longer than SCTH (2.5 min UC pulses). At about 0.11–0.13 mol of H-donor, these three treatments have similar results, but consuming proportionally higher amounts of energy.

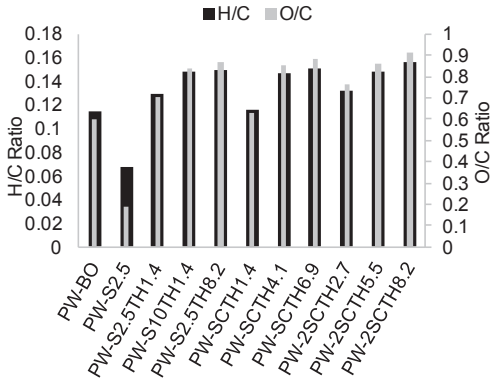


**Fig. 5.** H/C and O/C ratios after S, STH, SCTH, and 2SCTH treatments.

### 3.3. Spectroscopy analysis

Typical NMR spectra are presented in Fig. 6, which are similar to prior reported results [40,41]. The first observation is the presence of a signal attributed to ammonium formate in some of spectra. NMR spectra of blank solutions of H-donor were recorded as reference, and include untreated aqueous and sono-treated (e.g., water, methanol, and water/methanol) solutions in the presence of 0.5 g of Pd/C catalyst (as presented in Table S2 of Supplementary Information). The presence of ammonium formate signal in some of samples indicates that not all H-donor molecules decomposed under the applied conditions. This is particularly important for samples in which H-donor is added in higher amounts.

**Table 5**
Elemental composition of untreated and treated bio-oil samples (dry/ash-free basis).

| Sample ID | Carbon (%w/w) | Hydrogen (%w/w) | Nitrogen (%w/w) | Oxygen (%w/w) | Sulfur (%w/w) |
|---|---|---|---|---|---|
| PW-BO | 58.12 | 6.65 | 0.32 | 34.91 | 0.02 |
| PW-S2.5 | 79.20 | 5.30 | 0.31 | 15.19 | 0.02 |
| PW-S2.5TH1.4 | 53.93 | 6.96 | 1.15 | 37.95 | 0.02 |
| PW-S10TH1.4 | 48.46 | 7.20 | 3.76 | 40.58 | 0.00 |
| PW-S2.5TH8.2 | 46.93 | 6.99 | 5.57 | 40.58 | 0.02 |
| PW-S2.5CTH1.4 | 56.60 | 6.55 | 1.14 | 35.67 | 0.02 |
| PW-S2.5CTH4.1 | 48.57 | 7.10 | 2.72 | 41.58 | 0.00 |
| PW-S2.5CTH6.9 | 46.87 | 7.08 | 4.74 | 41.29 | 0.00 |
| PW-2S5CTH2.7 | 51.65 | 6.84 | 2.07 | 39.39 | 0.02 |
| PW-2S5CTH5.5 | 47.82 | 7.12 | 3.77 | 41.25 | 0.02 |
| PW-2S5CTH8.2 | 45.59 | 7.10 | 5.75 | 41.57 | 0.00 |
| CS-BO | 51.93 | 7.42 | 0.87 | 39.65 | 0.05 |
| CS-S10C | 53.27 | 6.60 | 0.95 | 39.03 | 0.05 |
| CS-S10CTH1.4 | 52.18 | 7.44 | 2.18 | 38.08 | 0.05 |
| CS-S10TH1.4 | 51.14 | 7.48 | 2.17 | 39.08 | 0.05 |

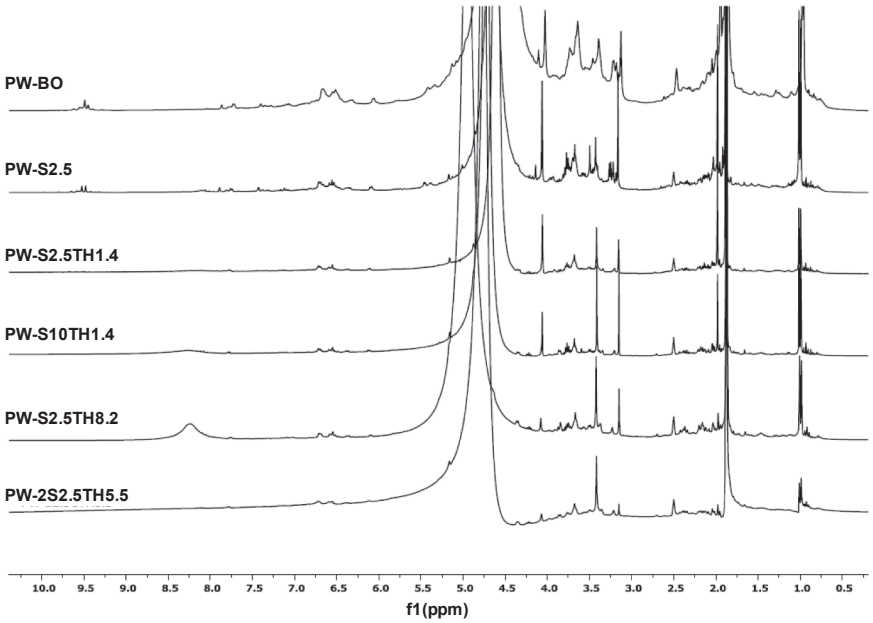


**Fig. 6.** Typical NMR spectra of untreated and treated bio-oil samples.

H-NMR spectroscopy was conducted to assess H-incorporation in the organic phase, including additional blank and controlled samples in water, methanol, and water:methanol (50:50 ratio) mix-solvent. The results indicate that neither total solubility increases in treatment duration, nor the presence of catalyst were separately or concertedly enough to cause the total decomposition of ammonium formate, whose signal was observed in all spectra. The donation reaction seemed to be a more powerful driver for the decomposition to occur. Assessing the absolute values of integrated areas or total integrated area showed no direct correlation with the absolute water content, nor to hydrogen content. Also, the comparison of total organic integrated (TOI) area (i.e., the total integrated area minus the water peak (5.0 ppm) area) with bio-oil [H] showed no direct correlation. However, the correlation between TOI and normalized TOI in terms of [H] is polynomial (Eq. (1)) and exhibits an $R^2 = 0.981$ (Fig. 7).

$$\boldsymbol{TOI} = -\mathbf{0.638}[\boldsymbol{TOI}/[\boldsymbol{H}]]^2 + \mathbf{13.39}[\boldsymbol{TOI}/[\boldsymbol{H}]] - \mathbf{15.32} \quad (1)$$

After the normalization of individual signals, the trend becomes more consistent. The application of sono-treatment (PW-S2.5) causes a decrease in the normalized intensity of all H-signals (Fig. 8). For STH treatments, substantial increases in the normalized intensity of signals for α-aliphatic protons closed to heteroatoms or unsaturation are observed in cases where the ammonium formate signal is absent. The ether and methoxyl groups signals are also highly affected. These results indicate the incorporation of hydrogen to specific functional groups present in bio-oil compounds.

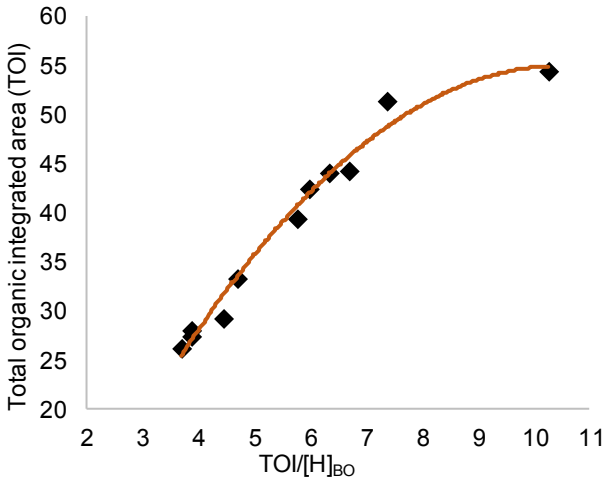


**Fig. 7.** NMR results from bio-oil protons.

### 3.4. *In-line spectroscopy analysis, multivariate calibration, and prediction modeling*

NIR spectra of 13 bio-oil samples were measured, using a spectroradiometer probe from 350 to 2500 nm. Three spectra were acquired per sample, and a mean spectrum was derived. Due to excessive noise from 350 to 550 nm, 850 to 1000 nm, and 2300 to 2500 nm, and spurious spectral responses at 1000 and 1800 nm, the wavelength region from 1050 to 1795 nm was used (Fig. 9). Seven properties were measured per sample (analyte values), presented in Table 3. Hydrogen, oxygen, and carbon values were used to evaluate H/C and O/C ratios on nine analytes.

PLS and RR methods have been used to form calibration models for each analyte, and LOOCV has been used to evaluate analyte prediction quality due to the limited number of samples. When the number of samples are limited, it becomes difficult for PLS to form effective models [42], however, RR often forms more effective models. With LOOCV, a sample was removed, leaving 12 samples to form and select respective PLS and RR models to predict the validation sample left-out of the corresponding calibration. For LOOCV and with mean centering, only 11 latent variables (LVs) models could be formed. For each cross-validation (CV), the calibration set was mean-centered, and the left-out validation sample was mean-centered to calibration mean. The final number of PLS LVs and RR parameters were selected, using U-curves based on all the calibration sample sets from LOOCV. PLS U-curves were formed by range scaling the mean root-mean-square-error of calibration (RMSEC) across 11 LVs from each CV, and adding these values to the range scaled mean jaggedness of respective regression vectors. The second U-curve was also formed by replacing the mean RMSEC with the mean $1\text{-}R^2$ where $R^2$ was obtained from plotting the calibration $\hat{y}$ (predicted values) against y (valid reference values) for each CV. LV at the minimum of the overall mean U-curve is used as the final model. RR U-curves were

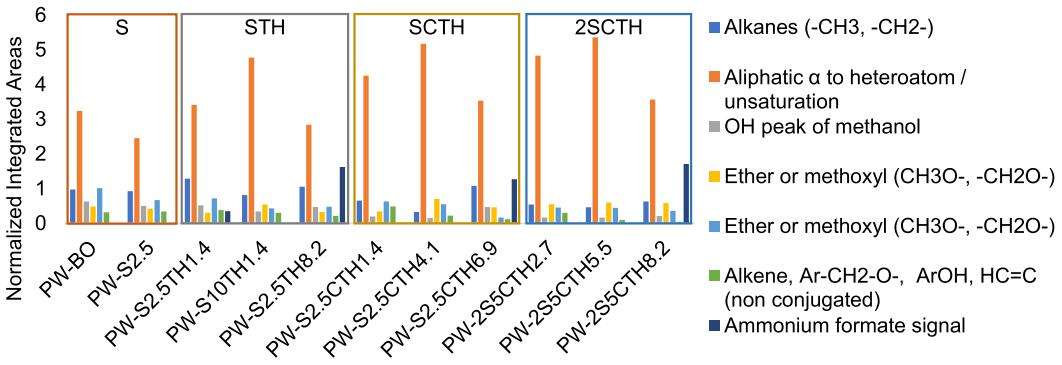


**Fig. 8.** Effect of treatments on H-NMR spectral signals.

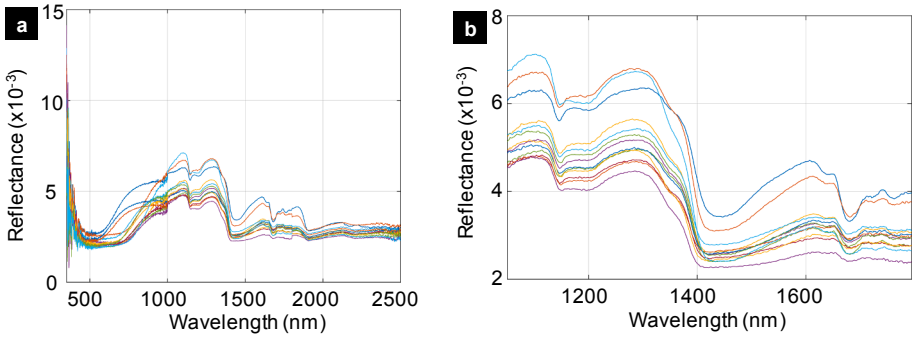


**Fig. 9.** (a) Sample mean full spectra of bio-oil between 350 and 2500 nm and (b) mean spectra over wavelength range used with PLS and RR between 1050–1795 nm.

formed the same as for PLS, using 50 ridge parameter values, ranging from 20.78 to 1.24e-6. Measures used to evaluate model quality were prediction errors for each sample left-out (RMSECV), $R^2$, slope, and intercept values from plotting $\hat{y}$ against y (Table 6).

## 4. Conclusions

This study proposed a process for bio-oil production and upgrading from two different biomass feedstocks (i.e., pinewood and corn stover). The conversion process employs a free-fall fast pyrolysis reactor combined with a fixed bed slow pyrolysis reactor for bio-oil and biochar production. The proposed SCTH upgrading approach includes four main processes, i.e., UC, CTH, STH, and SCTH, employing $NH_4HCO_2$ as hydrogen transfer additive and Pd/C as catalyst. Particularly, the overall effectiveness of the individual, and combined upgrading processes has been assessed by comparing the quality gains before and after bio-oil treatment. Additionally, this study proposed an in-line characterization approach, using a portable NIR spectroradiometer, multivariate calibration, and prediction modeling that enables the real-time analysis of the untreated and treated bio-oil quality (H/C and O/C ratios) to modify the process configuration (temperature and pressure) and improve the unit operation. The results indicate that H/C ratio is upgraded while O/C ratio is downgraded under STH and SCTH. Besides, the variation in the hydrogen contents cannot be directly caused by the decomposition of hydrogen-donor compound, but rather by a combined effect of carbon rejection and hydrogen incorporation in the organic phase. The second pass of SCTH treatment (2SCTH) showed that further upgrading beyond that achieved from primary experiments is less likely, except for the lowest H-donor addition. Although similar results can be achieved either by STH or SCTH, it is clear that energy intensification is gained with the presence of a catalyst. It is also apparent that STH treatments can only leverage SCTH treatments at higher H-donor concentration that will, in turn, represent an increase in operating costs.

The potential paths for future research activities are as follows:

- Development and implementation of quenching and stripping processes that can improve the sticky nature and instability of bio-oil.
- Exploration of molecular effects of STH and SCTH treatments for deeper and expanded upgrading investigation and guide its full development.

**Table 6**
Multivariate analysis results, using PLS and RR methods.

| Analyte | Partial Least Squares (PLS) | | | | | Ridge Regression (RR) | | | | |
|---|---|---|---|---|---|---|---|---|---|---|
| | No. LVs | RMSECV | $R^2$ | Slope | Intercept | Ridge Parameter | RMSECV | $R^2$ | Slope | Intercept |
| Moisture | 5 | 5.29 | 0.72 | 0.97 | 0.644 | 0.0010 | 3.57 | 0.84 | 0.897 | 4.63 |
| Carbon | 4 | 2.00 | 0.873 | 0.890 | 2.77 | 0.0010 | 1.93 | 0.89 | 0.817 | 4.36 |
| Hydrogen | 5 | 0.29 | 0.728 | 0.716 | 2.63 | 0.0010 | 0.26 | 0.77 | 0.690 | 2.85 |
| Nitrogen | 5 | 1.34 | 0.046 | 0.303 | 1.01 | 0.0007 | 1.20 | 0.00 | 0.042 | 1.43 |
| Oxygen | 5 | 2.03 | 0.839 | 0.896 | 6.78 | 0.0010 | 1.52 | 0.90 | 0.919 | 5.11 |
| Sulfur | 5 | 0.0099 | 0.238 | 0.680 | 0.002 | 0.0007 | 0.007 | 0.26 | 0.465 | 0.003 |
| Ash | 4 | 0.218 | 0.127 | 0.353 | 0.078 | 0.0010 | 0.20 | 0.11 | 0.259 | 0.092 |
| H/C ratio | 5 | 0.0512 | 0.740 | 0.852 | 0.058 | 0.0010 | 0.035 | 0.86 | 0.837 | 0.061 |
| O/C ratio | 5 | 0.404 | 0.733 | 0.894 | 0.282 | 0.0010 | 0.263 | 0.87 | 0.880 | 0.308 |

- Exploration of more systematic measurements to facilitate the proposed in-line characterization for real-time quality assessment and operation improvement.

## Author contributions

E.S, S.H., and A.M. performed the laboratory experiments; E.S., S.H., A.M., and M.M.R.C. analyzed the data and wrote the paper. Others contributed to the conceptual development and experimental design, as well as revised the manuscript.

## Funding sources

Equipment and Infrastructure Support (EIS) Grant from University of Idaho.

## Declaration of Competing Interest

The authors declare that they have no known competing financial interests or personal relationships that could have appeared to influence the work reported in this paper.

## Acknowledgments

The authors wish to acknowledge the financial support from University of Idaho, Equipment and Infrastructure Support (EIS) Grant and technical inputs by Dr. Haiyan Zhao and Mr. Kyler Beck on the catalyst transfer hydrogenation and spectroscopy analysis, as well as Center for Advanced Energy Studies (CAES) and Idaho National Laboratory (INL) for resources and facilities.

## Appendix A. Supplementary data

Supplementary data to this article can be found online at https://doi.org/10.1016/j.ultsonch.2021.105502.

## References

[1] U.S. Energy Information Administration (EIA) 2019. https://www.eia.gov.
[2] S. Hansen, A. Mirkouei, L.A. Diaz, A comprehensive state-of-technology review for upgrading bio-oil to renewable or blended hydrocarbon fuels, Renew. Sustain. Energy Rev. 118 (2020), 109548, https://doi.org/10.1016/j.rser.2019.109548.
[3] A. Mirkouei, K.R. Haapala, J. Sessions, G.S. Murthy, A review and future directions in techno-economic modeling and optimization of upstream forest biomass to bio-oil supply chains, Renew. Sustain. Energy Rev. 67 (2017) 15–35.
[4] W.-H. Chen, B.-J. Lin, M.-Y. Huang, J.-S. Chang, Thermochemical conversion of microalgal biomass into biofuels: a review, Bioresour. Technol. 184 (2015) 314–327.
[5] J.L. Easterly, Assessment of bio-oil as a replacement for heating oil, Northeast Reg. Biomass Program 1 (2002) 1–15.
[6] K. Jacobson, K.C. Maheria, D.A. Kumar, Bio-oil valorization: A review, Renew. Sustain. Energy Rev. 23 (2013) 91–106, https://doi.org/10.1016/j.rser.2013.02.036.
[7] M.M. Ramirez-Corredores, V. Sanchez, Challenges on the Quality of Biomass Derived Products for Bringing Them into the Fuels Market, J. Energy Power Eng. 6 (2012).
[8] B. Li, L. Ou, Q. Dang, P. Meyer, S. Jones, R. Brown, et al., Techno-economic and uncertainty analysis of in situ and ex situ fast pyrolysis for biofuel production, Bioresour. Technol. 196 (2015) 49–56, https://doi.org/10.1016/j.biortech.2015.07.073.
[9] A. Oasmaa, T. Sundqvist, E. Kuoppala, M. Garcia-Perez, Y. Solantausta, C. Lindfors, et al., Controlling the phase stability of biomass fast pyrolysis bio-oils, Energy Fuels 29 (2015) 4373–4381.
[10] A. Mirkouei, K.R. Haapala, J. Sessions, G.S. Murthy, A mixed biomass-based energy supply chain for enhancing economic and environmental sustainability benefits: A multi-criteria decision making framework, Appl. Energy 206 (2017) 1088–1101, https://doi.org/10.1016/j.apenergy.2017.09.001.
[11] A. Mirkouei, P. Mirzaie, K.R. Haapala, J. Sessions, G.S. Murthy, Reducing the cost and environmental impact of integrated fixed and mobile bio-oil refinery supply chains, J. Clean Prod. 113 (2016) 495–507.
[12] A.V. Bridgewater, Biomass fast pyrolysis, Therm. Sci. 8 (2004) 21–50.
[13] J. Lehto, Determination of kinetic parameters for Finnish milled peat using drop tube reactor and optical measurement techniques, Fuel 86 (2007) 1656–1663.
[14] C.J. Ellens, R.C. Brown, Optimization of a free-fall reactor for the production of fast pyrolysis bio-oil, Bioresour. Technol. 103 (2012) 374–380, https://doi.org/10.1016/j.biortech.2011.09.087.
[15] N. Punsuwan, C. Tangsathitkulchai, Product characterization and kinetics of biomass pyrolysis in a three-zone free-fall reactor, Int. J. Chem. Eng. 2014 (2014).
[16] E. Struhs, A. Mirkouei, Y. You, A. Mohajeri, Techno-economic and environmental assessments for nutrient-rich biochar production from cattle manure: A case study in Idaho, USA, Appl. Energy 279 (2020), 115782, https://doi.org/10.1016/j.apenergy.2020.115782.
[17] D. Mohan, U. Pittman Charles, P.H. Steele, Pyrolysis of Wood/Biomass for Bio-oil: A Critical Review, Energy Fuels 20 (2006) 848–889, https://doi.org/10.1021/ef0502397.
[18] Ramirez-Corredores MM, Iglesias VS. Production of renewable biofuels. US8968670B2, 2015.
[19] M.M. Ramirez-Corredores, J. Sorrells, C. Zhang, Production of renewable bio-distillate, US9062264B2 (2013).
[20] J. Tao, L. Liu, P. Zhu, K. Zhai, Q. Ma, D. Zhang, et al., Dual-template synthesis of cage-like Ni-based catalyst for hydrotreatment of bio-oil, J. Porous Mater. 26 (2019) 819–828.
[21] S. Hansen, A. Mirkouei. Bio-Oil Upgrading Via Micro-Emulsification And Ultrasound Treatment: Examples For Analysis And Discussion. ASME 2019 Int. Des. Eng. Tech. Conf. Comput. Inf. Eng. Conf., 2019.
[22] M.K. Anwer, D. Sherman, J.G. Roney, A.F. Spatola, Applications of ammonium formate catalytic transfer hydrogenation. 6. Analysis of catalyst, donor quantity, and solvent effects upon the efficacy of dechlorination, J. Org. Chem. (1989), https://doi.org/10.1021/jo00267a012.
[23] S.-K. Yang, P.-G. Duan, Effect of ultrasonic pretreatment on the properties of bio-oil, Energy Sources Part Recovery Util. Environ. Eff. 39 (2017) 941–945, https://doi.org/10.1080/15567036.2016.1277285.
[24] R. Gopinath, A.K. Dalai, J. Adjaye, Effects of Ultrasound Treatment on the Upgradation of Heavy Gas Oil, Energy Fuels 20 (2006) 271–277, https://doi.org/10.1021/ef050231x.
[25] L. Qin, Y. Shao, Z. Hou, Y. Jia, E. Jiang, Ultrasonic-Assisted Upgrading of the Heavy Bio-Oil Obtained from Pyrolysis of Pine Nut Shells with Methanol and Octanol Solvents, Energy Fuels 33 (2019) 8640–8648, https://doi.org/10.1021/acs.energyfuels.9b01248.
[26] A. Asiedu, R. Davis, S. Kumar, Catalytic transfer hydrogenation and characterization of flash hydrolyzed microalgae into hydrocarbon fuels production (jet fuel), Fuel 261 (2020), 116440.
[27] P. Panagiotopoulou, D.G. Vlachos, Liquid phase catalytic transfer hydrogenation of furfural over a Ru/C catalyst, Appl. Catal. Gen. 480 (2014) 17–24, https://doi.org/10.1016/j.apcata.2014.04.018.
[28] S.V. Sancheti, P.R. Gogate, Ultrasound assisted selective catalytic transfer hydrogenation of soybean oil using 5% Pd/C as catalyst under ambient conditions in water, Ultrason. Sonochem. 38 (2017) 161–167, https://doi.org/10.1016/j.ultsonch.2017.03.004.
[29] J.L. Pinilla, A.B. García, K. Philippot, P. Lara, E.J. Garcia-Suarez, M. Millan, Carbon-supported Pd nanoparticles as catalysts for anthracene hydrogenation, Fuel 116 (2014) 729–735.
[30] Z. Wu, N. Cherkasov, G. Cravotto, E. Borretto, A.O. Ibhadon, J. Medlock, et al., Ultrasound- and Microwave-Assisted Preparation of Lead-Free Palladium Catalysts: Effects on the Kinetics of Diphenylacetylene Semi-Hydrogenation, ChemCatChem 7 (2015) 952–959, https://doi.org/10.1002/cctc.201402999.
[31] J. Luo, Z. Fang, R.L. Smith, Ultrasound-enhanced conversion of biomass to biofuels, Prog. Energy Combust. Sci. 41 (2014) 56–93, https://doi.org/10.1016/j.pecs.2013.11.001.
[32] R. Sivaramakrishnan, A. Incharoensakdi, Microalgae as feedstock for biodiesel production under ultrasound treatment – A review, Bioresour. Technol. 250 (2018) 877–887, https://doi.org/10.1016/j.biortech.2017.11.095.
[33] S. De, B. Saha, R. Luque, Hydrodeoxygenation processes: Advances on catalytic transformations of biomass-derived platform chemicals into hydrocarbon fuels, Bioresour. Technol. 178 (2015) 108–118.
[34] H.P. Reddy Kannapu, C.A. Mullen, Y. Elkasabi, A.A. Boateng, Catalytic transfer hydrogenation for stabilization of bio-oil oxygenates: Reduction of p-cresol and furfural over bimetallic Ni–Cu catalysts using isopropanol, Fuel Process Technol. 137 (2015) 220–228, https://doi.org/10.1016/j.fuproc.2015.04.023.
[35] J.H. Kalivas, R.L. Green, Pareto optimal multivariate calibration for spectroscopic data, Appl. Spectrosc. 55 (2001) 1645–1652.
[36] J.H. Kalivas, J. Palmer, Characterizing multivariate calibration tradeoffs (bias, variance, selectivity, and sensitivity) to select model tuning parameters, J. Chemom. 28 (2014) 347–357.
[37] A.A. Gowen, G. Downey, C. Esquerre, C.P. O'Donnell, Preventing over-fitting in PLS calibration models of near-infrared (NIR) spectroscopy data using regression coefficients, J. Chemom. 25 (2011) 375–381.
[38] A.V. Bridgwater, Review of fast pyrolysis of biomass and product upgrading, Biomass Bioenergy 38 (2012) 68–94, https://doi.org/10.1016/j.biombioe.2011.01.048.
[39] M.M. Ramirez-Corredores, The science and technology of unconventional oils: finding refining opportunities, Academic press, 2017.
[40] C.A. Mullen, G.D. Strahan, A.A. Boateng, Characterization of various fast-pyrolysis bio-oils by NMR spectroscopy, Energy Fuels 23 (2009) 2707–2718.
[41] N. Hao, H. Ben, C.G. Yoo, S. Adhikari, A.J. Ragauskas, Review of NMR characterization of pyrolysis oils, Energy Fuels 30 (2016) 6863–6880.
[42] P. Shahbazikhah, J.H. Kalivas, A consensus modeling approach to update a spectroscopic calibration, Chemom. Intell. Lab. Syst. 120 (2013) 142–153.